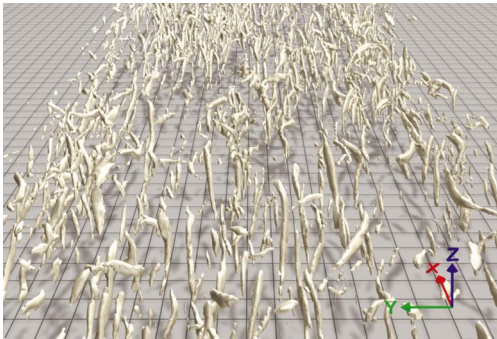
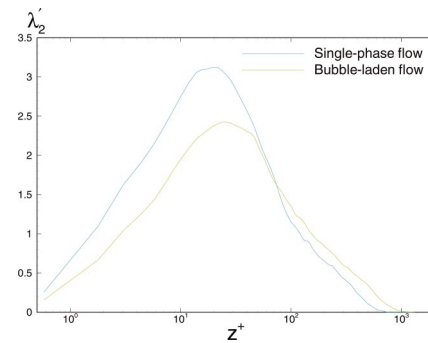
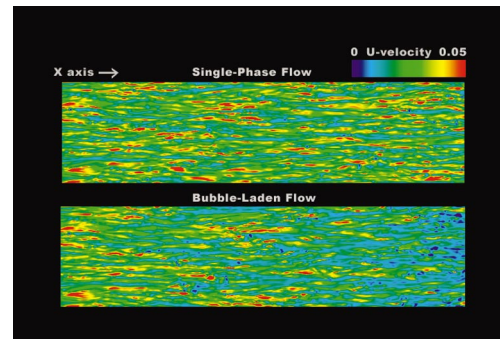


FIG. 1. Single-phase flow: vortical structures at  $t=60$ .FIG. 2. Bubble-laden flow: vortical structures at  $t=60$ .FIG. 3. Root-mean square of  $\lambda_2$  at  $x=18.8\delta_0$ .FIG. 4. Wall streaks: contours of the instantaneous ( $t=60$ ) streamwise fluid velocity in the horizontal  $xy$ -plane at  $z^+=0.58$ .

## Evolution of Quasistreamwise Vortex Tubes and Wall Streaks in a Bubble-laden Turbulent Boundary Layer over a Flat Plate

Submitted by

A. Ferrante and S. Elghobashi, University of California, Irvine

P. Adams, M. Valenciano, and D. Longmire, U.S. Army Engineer Research and Development Center

Ferrante and Elghobashi<sup>1</sup> performed direct numerical simulation (DNS) of microbubble-laden spatially developing turbulent boundary layer over a flat plate to explain the fundamental physical mechanisms responsible for the reduction of skin-friction due to the presence of the microbubbles.

Here, we present flow visualizations obtained from the above-mentioned DNS data.<sup>1,2</sup> The spatially developing turbulent boundary layer (of liquid water) is laden with gaseous air microbubbles (bubble diameter in wall units  $d_b^+ = 2.4$ ) at an average volume fraction  $\phi_v = 0.02$ . The gravitational acceleration is perpendicular to and oriented towards the plate (“plate-on-bottom,” case E in Refs. 1 and 2). Our DNS results for the bubble-laden flow are compared with those for the single-phase flow ( $1020 \leq \text{Re}_\theta \leq 1480$ , case A in Refs. 1 and 2).

Figures 1 and 2 display the instantaneous surfaces of the quasistreamwise vortical structures at time  $t=60$ . These structures are identified<sup>3</sup> as connected flow regions of nega-

tive values of  $\lambda_2$ , where  $\lambda_2$  is the second largest eigenvalue of the tensor  $(S_{ik}S_{kj} + \Omega_{ik}\Omega_{kj})$ ;  $S_{ij} \equiv (\partial_j U_i + \partial_i U_j)/2$  is the strain rate tensor, and  $\Omega_{ij} \equiv (\partial_j U_i - \partial_i U_j)/2$  is the rotation rate tensor. The depicted structures are for  $\lambda_2 = -4$ . The vortical structures (Figs. 1 and 2) sometimes appear as asymmetric *horseshoes* or *hairpins*. However, in the bubble-laden flow, the generated *velocity divergence*<sup>1,2</sup> induces a wall-normal fluid velocity that displaces the vortical structures away from the wall, to a region of smaller mean shear. Consequently, the peak of the root-mean square of  $\lambda_2$  is displaced about five wall units away from the wall, and the intensity of the vortical structures is reduced near the wall ( $z^+ < 75$ ), as shown in Fig. 3. The displacement of the vortical structures increases the spanwise gaps between the *wall streaks* associated with the *sweep events* (red regions in Fig. 4), and reduces the streamwise velocity in these streaks in comparison to that of the single phase flow as shown in Fig. 4, thus reducing the skin friction by up to 14% for plate-on-bottom and 20% for plate-on-top for  $\phi_v = 0.02$ .

<sup>1</sup>A. Ferrante and S. Elghobashi, “On the physical mechanisms of drag reduction in a spatially developing turbulent boundary layer laden with microbubbles,” *J. Fluid Mech.* **503**, 345 (2004).

<sup>2</sup>A. Ferrante, “Reduction of skin-friction in a microbubble-laden spatially developing turbulent boundary layer over a flat plate,” Ph.D. thesis, University of California, Irvine, 2004.

<sup>3</sup>J. Jeong and F. Hussain, “On the identification of a vortex,” *J. Fluid Mech.* **285**, 69 (1995).